Discover Oncology

Research

Interfered long non-coding RNA HELLPAR or up-regulated microRNA-448 inhibits nasopharyngeal carcinoma progression via suppression of ADAM10

Wenjuan Zhu[1] · Qi Yang[1] · Huijun Yang[1] · Mingtao Qian[1] · Yan Ji[1] · Jianyong Liu[1]

Received: 8 February 2025 / Accepted: 5 May 2025
Published online: 21 May 2025

Abstract

Objective Nasopharyngeal carcinoma (NPC) is a highly invasive malignancy with poor prognosis, necessitating further exploration of its molecular mechanisms. While HELLP-associated long non-coding RNA (HELLPAR), microRNA-448 (miR-448), and a disintegrin and metalloprotease 10 (ADAM10) have been implicated in other malignancies, their regulatory interplay and functional roles in NPC remain unclear. This study aimed to investigate the role of HELLPAR in NPC progression through its interaction with miR-448 and ADAM10.

Methods Cancerous and adjacent non-cancerous tissues were collected from 53 NPC patients admitted to our hospital between 1st January 2018 and 1st January 2020. Transcript levels of HELLPAR, miR-448, and ADAM10 were measured using quantitative real-time PCR (RT-qPCR), while the protein expression levels of ADAM10 were assessed by Western blotting. Long-term survival data were analyzed to assess the correlation between HELLPAR expression and patient prognosis. The binding interactions of HELLPAR/miR-448 and miR-448/ADAM10 were predicted and experimentally validated. Overexpression and knockdown constructs for HELLPAR, miR-448, and ADAM10 were transfected into NPC cells to assess their effects on proliferation, invasion, and apoptosis.

Results HELLPAR and ADAM10 were significantly upregulated at both the RNA and protein levels in NPC tissues and cells, while miR-448 was notably downregulated. Suppression of HELLPAR inhibited NPC cell proliferation and invasion while promoting apoptosis. Mechanistically, HELLPAR functioned as a competitive endogenous RNA (ceRNA) by binding to miR-448, thereby downregulating its RNA expression. Overexpression of miR-448 counteracted the tumor-promoting effects of HELLPAR. Additionally, miR-448 directly targeted and suppressed ADAM10. Overexpression of ADAM10 reversed the inhibitory effects of miR-448 on NPC cell proliferation and invasion.

Conclusion The HELLPAR/miR-448/ADAM10 axis plays a critical role in NPC progression. Suppressing HELLPAR expression enhances miR-448 activity, which in turn downregulates ADAM10 at both RNA and protein levels, leading to reduced NPC cell proliferation and invasion while promoting apoptosis.

Keywords Long non-coding RNA HELLPAR · MicroRNA-448 · A disintegrin and metalloprotease 10 · Nasopharyngeal carcinoma · Invasion · Apoptosis · Proliferation

✉ Jianyong Liu, Liujianyong6199@163.com | [1]Otolaryngology Head and Neck Surgery, Zhangjiagang Hospital Affiliated to Soochow University (Zhang Jiagang First Peoples Hospital), No. 68, West Jiyang Road, Zhangjiagang 215600, Jiangsu, China.

1 Introduction

Nasopharyngeal carcinoma (NPC), a subtype of head and neck cancer, originates from the epithelial lining of the nasopharynx [1]. NPC exhibits a distinct geographical distribution and is particularly prevalent in East and Southeast Asia [2]. It is a malignancy closely related to Epstein-Barr virus infection [3]. Magnetic resonance imaging is commonly employed for the diagnosis and grading of NPC, and endoscopic biopsy remains the gold standard for pathological confirmation [4]. Radiotherapy is the primary treatment modality for NPC [5]. Although early-stage NPC can be effectively managed with a combination of radiotherapy and chemotherapy, the prognosis for patients with recurrent or metastatic disease remains poor [6]. Therefore, it is imperative to explore novel treatment strategies that can effectively promote survival in patients with NPC.

Long non-coding RNAs (LncRNAs) are a group of non-protein coding RNA molecules that have emerged as critical regulators in various cancers, including NPC. Many functional lncRNAs exert their roles by interacting with microRNAs (miRNAs) and proteins, forming complicated regulatory networks [7]. For example, HELLPAR (HELLP associated lncRNA) has been reported to be linked to cell cycle and apoptosis during the prostate cancer progression [8]. miRNAs refer to a class of endogenous, short-stranded, non-coding RNAs of 19–22-nucleotide length. They could transcriptionally suppress or degrade themselves to modulate post-transcriptional gene expression [9, 10]. miRNAs have been extensively investigated for their capability in the diagnosis, prognosis, and treatment of human diseases [11], serving as crucial regulators of gene expression [12]. Among them, miR-448 has been shown to participate in tumor progression. For instance, one study has demonstrated that miR-448, along with other factors, impedes self-renewal and stemness maintenance of hepatocellular carcinoma (HCC) stem cells, identifying its therapeutic potential HCC treatment [13]. Additionally, miR-448 has been found to suppress gastric cancer progression [14], and its expression is lowly expressed in lung adenocarcinoma and gastric cancer tissues and cell lines [14]. A disintegrin and metalloprotease 10 (ADAM10) has also been identified as a contributor to NPC progression, with studies suggesting that its upregulation may facilitate tumor metastasis, making it a potential therapeutic target [15]. Inspired by these findings, we realized a significant knowledge gap regarding the role of HELLPAR in NPC. Therefore, this paper focused on ascertaining the HELLPAR/miR-448/ADAM10 axis on NPC progression.

2 Materials and methods

2.1 Ethical approval

The study conformed to the principles expressed in the *Declaration of Helsinki* and was approved by the Institutional Review Board of Zhangjiagang Hospital Affiliated to Soochow University (Zhang Jiagang First Peoples Hospital). All patients provided written informed consent.

2.2 Study subjects

Cancerous and paracancerous tissues (3 cm from the cancerous tissues) were obtained from 53 NPC patients admitted to the Oncology Department of Zhangjiagang Hospital Affiliated to Soochow University (Zhang Jiagang First Peoples Hospital) from 1 st January 2018 to 1 st January 2020. The paracancerous tissues were confirmed to be non-cancerous by pathological examination and were used as controls in the study. The patients had a mean age of 53.48 ± 4.15 years, and their general and pathological diagnostic data were collected. All patients underwent nasopharyngeal biopsy and were pathologically confirmed to have NPC, excluding those with recurrent NPC or other malignancies. All patients received radical radiotherapy. Telephone and outpatient follow-up was carried out for 60 months.

2.3 Cell culture, transfection, and treatment

Human NPC cell lines (HK-1, TW03, C666-1, and HNE-3) and the normal nasopharyngeal epithelial cell line NP69 were provided by the Shanghai Institutes for Biological Sciences, Chinese Academy of Sciences (Shanghai, China). The cells were cultivated at 37 ℃ in Roswell Park Memorial Institute-1640 medium containing 5% CO_2, 10% fetal bovine serum (FBS), 100 μg/mL penicillin, and 100 μg/mL streptomycin. Overexpression sequences for miR-448 and ADAM10 (oe-miRNA-448

and oe-ADAM10), as well as HELLPAR overexpression and knockdown sequences (oe-HELLPAR and sh-HELLPAR), along with corresponding control sequences were designed and synthesized by Sangon Biotech (Shanghai, China). Cell transfection was conducted using Lipofectamine 2000 reagent (Invitrogen, Carlsbad, CA, USA). After transfection, cells were incubated under 5% CO_2 for 48 h before following experiments.

2.4 Reverse transcription quantitative polymerase chain reaction (RT-qPCR)

TrizoL (Invitrogen) was utilized to extract total RNA from each group of cells. The OD value and RNA concentrations were assessed by a NanoDrop 2000 UV spectrophotometry (Thermo Fisher Scientific, USA). For miRNA detection, reverse transcription to generate cDNA was carried out using TaqMan MicroRNA Assays Reverse Transcription Primer (4,427,975, Applied Biosystems, USA). For mRNA, reverse transcription was performed with PrimeScript RT reagent Kit (RR047 A, Takara, Japan). Real-time PCR was conducted by SYBR® Green I. PCR primers were designed and synthesized by Invitrogen (Table 1). U6 served as the loading control of miR-448, and GAPDH for HELLPAR and ADAM10. Relative expression was calculated using the $2^{-\Delta\Delta Ct}$ method.

2.5 Western blot assay

ADAM10 protein levels in tissues and cells were assessed by western blotting. Tissues were placed in tubes, lysed with 100 µL of radioimmunoprecipitation assay lysis buffer (R0020, Soleberg, Beijing, China) containing 1 mmol/L phenylmethanesulfonyl fluoride, and homogenized at 3000 r/min until fully lysed. The lysates were then centrifuged at 12,000 g for 4 min, and the supernatants were preserved at −80℃. BCA kit (AR0146, BOSTER, Wuhan, Hubei, China) was employed to test protein concentration, and the concentration of samples was adjusted to 3 µg/µL. Proteins (30 µg/well) were mixed with sample buffer, boiled at 95 ℃, and separated by 10% SDS-PAGE. After electrophoresis, proteins were transferred to polyvinylidene fluoride (PVDF) membrane (P2438, Sigma, USA) via semi-dry electrotransfer membrane method, and blocked by 5% BSA (10-L16, Biopartner Science & Technology Co. Ltd., Beijing, China) at ambient temperature. Rabbit anti-ADAM10 (ab124695; 1:1000; Abcam, USA) was added and cultivated overnight at 4℃, followed by sheep anti-rabbit secondary antibodies (ab6721, 1:2000, Abcam. Chemiluminescent reagents were employed for detection, with GAPDH (ab9485; 1:1000; Abcam) serving as internal reference. Blots were visualized using the Bio-rad Gel Dol EZ imager (Bio-rad, California, USA), and band intensity was analyzed with Image J software (version 1.48; National Institutes of Health) [16].

2.6 CCK-8 assay

The successfully-transfected cells were digested with trypsin, centrifuged, resuspended in complete medium, and counted, followed by a continuous cultivation at 37℃ with 5% CO_2 for 4 days. The OD values were first assessed after overnight incubation. CCK-8 solution (10 µL) at 24 h, 48 h and 72 h was added and incubated. When the color of the solution changed from light red to yellow, the OD values at 490 nm were tested with a microplate reader (BIO-TEK USA). Finally, the cell growth curves were plotted according to the measured values [17].

Table 1 Primer sequence for RT-qPCR

Gene	Primer sequence (5′–3′)
HELLPAR	Forward: ACACCATTTTGAGTATCATAA
	Reverse: CAGTCAATCTGATAAGAGAG
MiR-448	Forward: GCGCGTTGCATATGTAGGATG
	Reverse: AGTGCAGGGTCCGAGGTATT
ADAM10	Forward: GGAGTGTACGTGTGCCAGTTCTG
	Reverse: GGTTCGACCACTGAAGTGCCTAC
U6	Forward: CAGCACATATACTAAAATTGGAACG
	Reverse: ACGAATTTGCGTGTCATCC
GAPDH	Forward: GGAGCGAGATCCCTCCAAAAT
	Reverse: GGCTGTTGTCATACTTCTCATGG

MiR-448, microRNA-448; ADAM10, a disintegrin and metalloprotease 10

2.7 Transwell assay

Transwell assay was implemented for assessing cell invasion, using Matrigel®-precoated Transwell®chamber (Corning). A total of 200 µL of transfected cells (5×10^4 cells/mL) from each group were inoculated into the matrix gel-coated upper chambers. After 24 h of incubation, the cells that migrated to the lower half were Giemsa-stained, and the invasion rate was calculated. DMI4000B microscope (Leica, Wetzlar, Germany) was employed to capture images, and 5 fields of view were randomly selected for cell counting [18, 19].

2.8 Flow cytometry

Cells were seeded into a 6-well plate and transfected. After 48 h, they were digested with 1 mL of trypsin and neutralized with 1 mL of medium. Cells were then centrifuged at 800 rpm, resuspended in 4 mL PBS, centrifuged again at 800 rpm, and finally resuspended in 500 mL Binding Buffer. Subsequently, the cells were incubated in the dark for 10 min with 5 µL of Annexin V-FITC (20 µg/mL) and 10 µL of PI solution (50 µg/mL). Flow cytometric analysis was performed using a Becton Dickinson flow cytometer within 1 h.

2.9 Nuclear and cytoplasmic separation assay

Cells were rinsed with cold PBS and centrifugal at 1000 rpm, followed by gentle resuspension and incubation on ice in 200 µL of lysis buffer A [Tris (10 mM, pH 8.0), NaCl (140 mM), $MgCl_2$ (1.5 mM) 0.5% Nordez P-40] for 5 min. After centrifugation at 1000 × g for 3 min at 4 °C the supernatants (cytoplasmic portions) were collected and mixed with RNAiso Reagent (1 mL). The remaining nuclear pellets were rinsed twice by utilizing lysis buffer A and lysis buffer A containing 1% Tween-40 and 0.5% deoxycholic acid, respectively. The nuclear pellets were then resuspended with RNAiso Reagent (1 mL). Subsequently, the cytoplasmic and nuclear RNA were purified and analyzed by RT-qPCR [20].

2.10 Luciferase detection assay

StarBase v3.0 (http://starbase.sysu.edu.cn/) was utilized to predict the potential binding sites between HELLPAR and miR-448, as well as the target binding sites of miR-448 within the 3'UTR region of ADAM10. The miRNA-lncRNA and miRNA-mRNA interaction modules in the StarBase database were utilized to identify these putative sequences. A dual-luciferase reporter gene assay was conducted to further verify the targeting relationship HELLPAR and miR-448, and to confirm ADAM10 as a direct target of miR-448. Based on the predicted binding regions, both wild-type (WT) and mutant (MUT) sequences of HELLPAR and the ADAM10 3'UTR were synthesized. The sequences were cloned into the pMIR-reporter vector (HUAYUEYANG Biotechnology, Beijing, China) using SpeI and HindIII restriction sites. Mutated sequences were processed via restriction enzyme digestion. The target fragments were ligated into the reporter plasmid using T4 DNA ligase. The luciferase reporter plasmids (WT and MUT) were then co-transfected with either miR-448 mimic or negative control (mimic-NC) into HEK-293 T cells. Luciferase activity was measured using the Dual-Luciferase Assay System (Promega, Madison, WI) on a Glomax 20/20 luminometer (Promega) [21].

2.11 RNA immunoprecipitation (RIP) assay

Cell lysis was performed using buffer containing 25 mM Tris–HCl (pH 7.4), 150 mM NaCl, 0.5% NP-40, 2 mM EDTA, 1 mM NaF, and 0.5 mM dithiothreitol, supplemented with RNasin (Takara) and a protease inhibitor cocktail (B14001a, Roche, USA). The lysates were centrifuged at 12,000 g, and the supernatant was incubated with anti-Ago2 magnetic beads (130–061–101, Shanghai Universal Biotech Co., Ltd.). Beads coated with anti-IgG were used as negative controls. After 4 h of incubation at 4 °C, the beads were washed with buffer containing 50 mM Tris–HCl, 300 mM NaCl (pH 7.4), 1 mM $MgCl_2$, and 0.1% NP-40. RNA was extracted using TRIzol, and HELLPAR enrichment was detected via RT-qPCR.

2.12 RNA pull-down assay

Cells were transfected with 50 nM of biotin-labeled miR-448-WT or miR-448-MUT (Wuhan Genecreate Biological Engineering Co., Ltd., Hubei, China). After 48 h, cells were lysed in a specialized buffer (Ambion, Austin, TX, USA) for 10 min. The lysates were then incubated overnight at 4 °C with M-280 streptavidin magnetic beads (S3762, Sigma, USA), pre-blocked with RNase-free BSA and yeast tRNA (TRNABAK-RO, Sigma, USA). Bound RNA was purified, and the enrichment of HELLPAR was analyzed [22].

2.13 Statistical analysis

All data were analyzed using SPSS 22.0 statistical software (SPSS, Inc, Chicago, IL, USA), and graphs were generated using GraphPad Prism 9.5 software (California, USA). Measurement data were depicted as mean ± standard deviation, and paired t-tests were employed for comparisons between cancerous and paracancerous tissues. Comparisons between two independent groups were conducted by independent samples t-tests, and comparisons of multiple groups were conducted by one-way analysis of variance (ANOVA) followed by Tukey's for post hoc tests. Repeated measures ANOVA with Bonferroni correction was used for time-series data between group. Statistically significant differences were defined as $P < 0.05$.

3 Results

3.1 HELLPAR is highly expressed in NPC tissues and cells and is associated with poor prognosis

As previously reported, HELLPAR is overexpressed in glioma [23], but no studies have yet investigated its expression in NPC. To explore HELLPAR expression in NPC, RT-qPCR was conducted. The findings (Fig. 1A) unraveled that HELLPAR was highly expressed in NPC tissues compared to matched paracancerous tissues. Similarly, in all examinied NPC cell lines (Fig. 1B), HELLPAR expression was higher than in normal nasopharyngeal epithelial NP69 cells, with the most prominent difference observed in HK-1 cells. Based on the median epression value of HELLPAR, patients were divided into low and high expression group. Kaplan–Meier analysis demonstrated that patients with high HELLPAR expression had significantly shorter survival than those with low HELLPAR expression ($P < 0.05$) (Fig. 1C). These findings unravel that HELLPAR is highly expressed in NPC and may serve as a prognostic indicator of poor clinical outcome.

3.2 Silencing HELLPAR suppresses NPC cell proliferative and invasive activities and promotes apoptosis

To investigate the biological role of HELLPAR in NPC, HK-1 cells were treated with sh-HELLPAR. Knockdown efficiency was confirmed by RT-qPCR (Fig. 2A). CCK-8 assay revealed a significant reduction in proliferative capacity upon HELLPAR silencing (Fig. 2B). Flow cytometry indicated that HELLPAR knockdown promoted apoptosis (Fig. 2C). Transwell assay

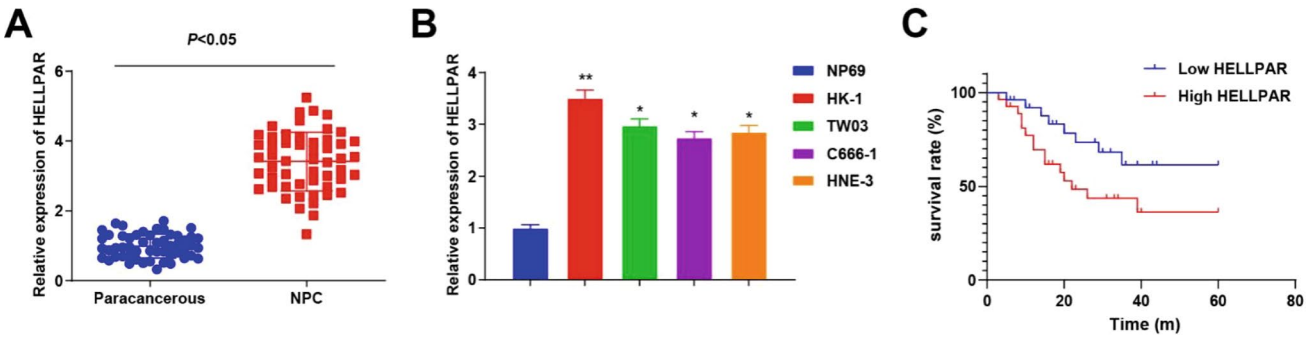

Fig. 1 Differential expression of HELLPAR in NPC tissues and cells. **A** HELLPAR expression levels in paracancerous tissues and NPC tissues were tested by RT-qPCR; **B** HELLPAR expression levels in NP69, HK-1, TW03, C666-1, and HNE-3 cells were assessed; **C** The relationship of HELLPAR expression and the survival of NPC patients was analyzed by Kaplan–Meier analysis; * $P < 0.05$, ** $P < 0.01$; N = 53

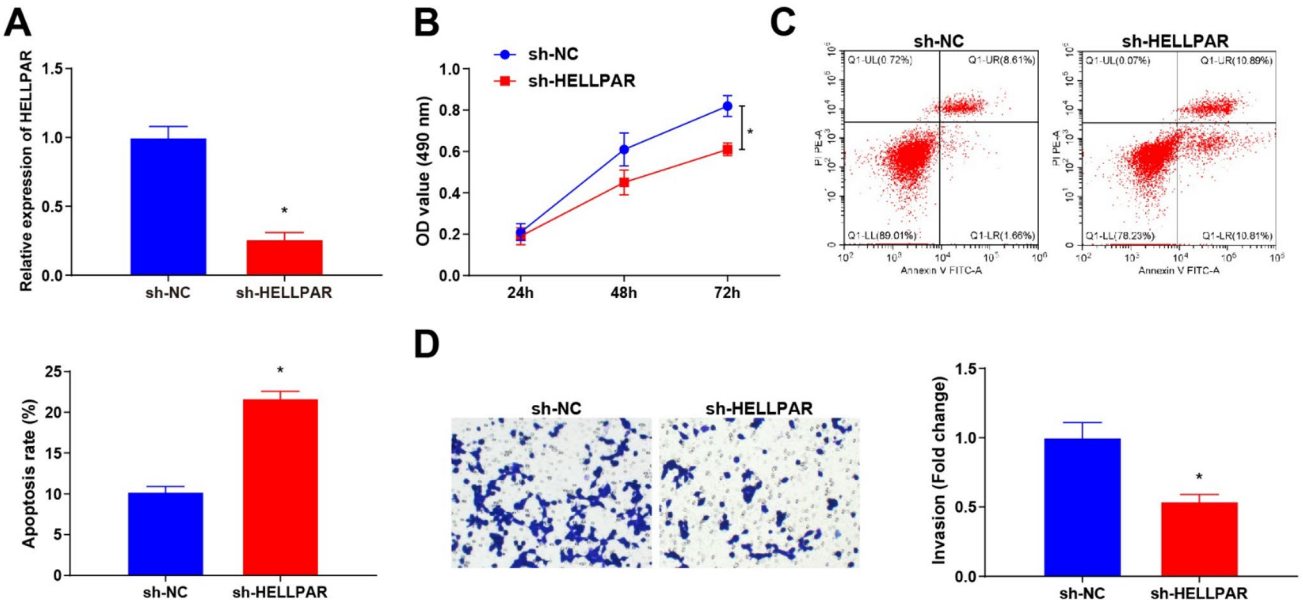

Fig. 2 HELLPAR expression influences the biological functions of NPC cells. **A**. HELLPAR interference efficiency in NPC cells was assessed by RT-qPCR; **B**. The proliferation ability of cells after sh-HELLPAR treatment was tested by CCK-8 assay; **C**. The apoptosis rate after sh-HELLPAR treatment was assessed by flow cytometry; **D**. The invasive ability of cells after sh-HELLPAR treatment was measured by Transwell assay; * $P < 0.05$ vs sh-NC

demonstrated a marked decrease in the invasive ability of sh-HELLPAR-treated cells (Fig. 2D). These results indicate that interfering HELLPAR impedes NPC cell proliferative and invasive activities and promotes apoptosis.

3.3 HELLPAR functions as a ceRNA by competitively binding to miR-448

To elucidate the downstream regulatory mechanism of HELLPAR in NPC, subcellular localization analysis revealed that HELLPAR was predominantly located in the cytoplasm (Fig. 3A), suggesting a potential role as a ceRNA. Previous studies have reported miR-448 downregulation in breast cancer [24], but its role in NPC remains uncharacterized. Bioinformatic prediction using StarBase identified a potential binding site between HELLPAR and miR-448 (Fig. 3B). Dual-luciferase

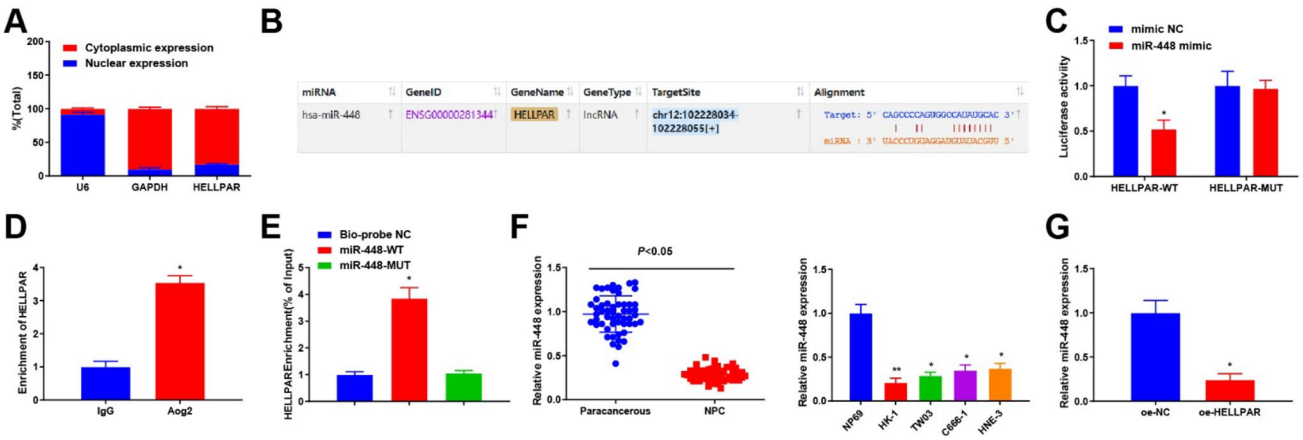

Fig. 3 HELLPAR competitively binds miR-448 and regulates its expression. **A**. The subcellular localisation of HELLPAR was observed by nuclear and cytoplasmic separation assay, with GAPDH as a cytoplasmic marker and U6 as a nuclear marker; **B**. Starbase website predicted the binding site of HELLPAR to miR-448; **C**. The binding of HELLPAR to miR-448 was verified by dual-luciferase assay; **D**. The binding of HELLPAR to miR-448 was tested by RIP assay; **E**: The enrichment of miR-448 for HELLPARRNA was measured by RNA pull-down assay; **F**. miR-448 expression in NPC tissues and cells was assessed by RT-qPCR; **G**. miR-448 expression after overexpression of HELLPAR was tested by RT-qPCR; * $P < 0.05$

reporter assay showed that miR-448 mimic significantly reduced luciferase activity in the HELLPAR-WT construct, but not in the mutant construct (Fig. 3C). RIP assay using anti-Ago2 antibody successfully pulled down HELLPAR (Fig. 3D), and RNA pull-down results further confirmed that HELLPAR was enriched in complexes with miR-448-WT, but not with miR-448-MUT (Fig. 3E), indicating a direct interaction. miR-448 expression was found to be significantly reduced in NPC tissues and cell lines (Fig. 3F), and was further suppressed following HELLPAR overexpression (Fig. 3G). Collectively, these results suggest that HELLPAR negatively regulates miR-448 by direct binding.

3.4 Overexpression of miR-448 reverses the oncogenic impacts of HELLPAR in NPC cells

To further address whether HELLPAR affected NPC cell biological functions through miR-448, the cells were grouped as follow: oe-NC + mimic-NC group, oe-HELLPAR + mimic-NC group, and oe-HELLPAR + miR-448 mimic group. RT-qPCR showed that versus the oe-NC + mimic-NC group, the oe-HELLPAR + mimic-NC group possessed diminished miR-448 expression levels; versus the oe-HELLPAR + mimic-NC group, the oe-HELLPAR + miR-448 mimic group possessed elevated miR-448 expression levels (Fig. 4A). Further functional assays revealed that versus the oe-NC + mimic-NC group, the cell proliferative and invasive capabilities were raised and the apoptosis rate was reduced in the oe-HELLPAR + mimic-NC group; compared with the oe-HELLPAR + mimic-NC group, the cell proliferative and invasive capabilities were decreased and the apoptosis rate was raised in the oe-HELLPAR + miR-448 mimic group (Fig. 4B–D). Taken together, miR-448 overexpression reverses the promoting effects of HELLPAR on NPC cell proliferative and invasive activities.

3.5 ADAM10 overexpression reverses the suppressive effects of miR-448 on NPC cells

miR-448's downstream target genes were further investigated. As previously reported, ADAM10 has a close relation to the survival of patients with tumors [25], but the specific mechanism remains unclear. In this study, a potential binding site between miR-448 and ADAM10 was predicted via the Starbase website (Fig. 5A). Meantime, we further found that (Fig. 5B) miR-448 targeted and regulated ADAM10. Moreover, ADAM10 expression was found to be highly expressed in both NPC tissues and cells (Fig. 5C) ($P < 0.05$).

Next, we explored whether miR-448 affected NPC cell biological functions through ADAM10. The cells were grouped as follow: mimic-NC + oe-NC group, miR-448 mimic + oe-NC group, and miR-448 mimic + oe-ADAM10 group. Western blot assay revealed that versus the mimic-NC + oe-NC group, the miR-448 mimic + oe-NC group possessed lower ADAM10 expression; versus the miR-448 mimic + oe-NC group, the miR-448 mimic + oe-ADAM10 group possessed higher ADAM10 expression (Fig. 5D). Further functional assays unraveled that compared with the mimic-NC + oe-NC group, cell

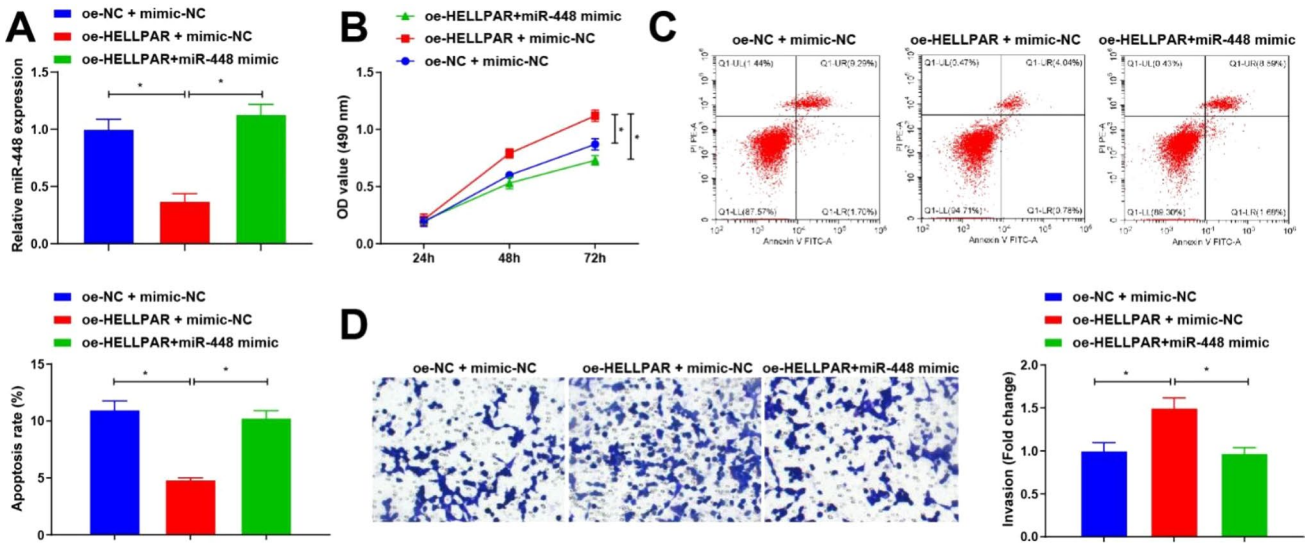

Fig. 4 HELLPAR sponges miR-448 to affect the biological functions of NPC cells. **A**. miR-448 expression after oe-HELLPAR + miR-448 mimic treatment was tested by RT-qPCR; **B**. The proliferation ability of cells after oe-HELLPAR + miR-448 mimic treatment was assessed by CCK-8 assay; **C**. The apoptosis rate after oe-HELLPAR + miR-448 mimic treatment was measured by flow cytometry; **D**. The invasive ability of cells after oe-HELLPAR + miR-448 mimic treatment was assessed by Transwell assay; * $P < 0.05$

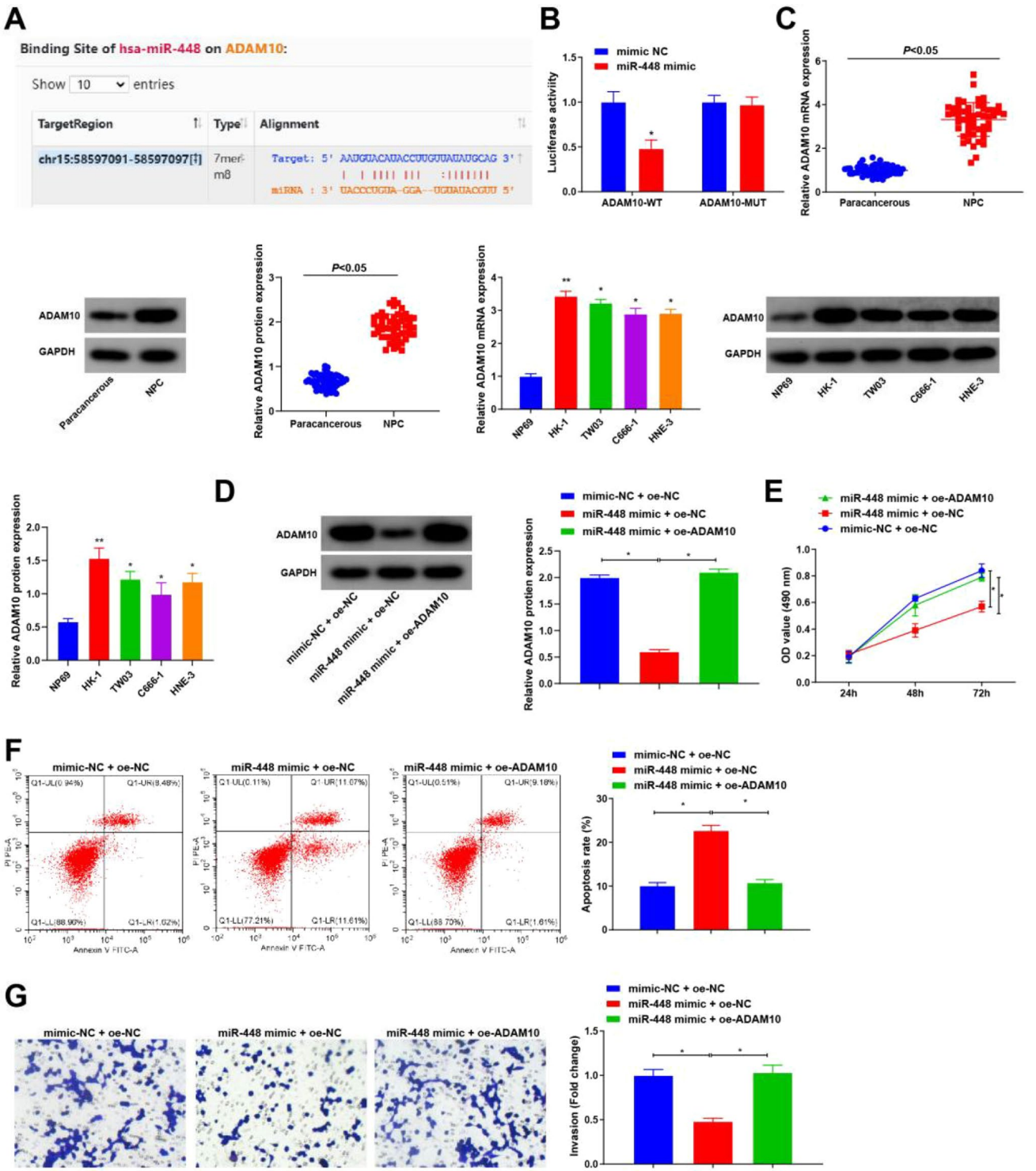

Fig. 5 miR-448 affects the biological functions of NPC cells by regulating ADAM10. **A**. Starbase website predicted the target binding site between miR-448 and ADAM10; **B**. The targeting relationship between miR-448 and ADAM10 was verified by dual-luciferase assay; **C**. ADAM10 expression in NPC tissues and cells was assessed by RT-qPCR and western blotting; **D**. ADAM10 expression in cells treated with miR-448 mimic + oe-ADAM10 was measured by western blotting; **E**. The proliferation ability of cells treated with miR-448 mimic + oe-ADAM10 was tested by CCK-8 assay; **F**. The apoptosis rate after treatment of miR-448 mimic + oe-ADAM10 was assessed by flow cytometry; **G**. The invasive ability of cells treated with miR-448 mimic + oe-ADAM10 was determined by Transwell assay; * $P < 0.05$

proliferative and invasive capability were decreased and the apoptosis rate was elevated in the miR-448 mimic + oe-NC group; versus the miR-448 mimic + oe-NC group, cell proliferative and invasive capability were raised and the apoptosis rate was diminished in the miR-448 mimic + oe-ADAM10 group (Fig. 5E-G). The above findings unravel that ADAM10 overexpression counteracts the inhibitory impacts of miR-448 on the proliferative and invasive activities of NPC cells.

4 Discussion

This study aimed to unveil the role of HELLPAR in NPC progression via the miR-448/ADAM10 axis. While the mechanism of miR-448 in NPC remains unclear, previous studies suggest its potential regulatory role in cancer biology. Additionally, ADAM10 has been implicated in promoting cell proliferation and invasion in NPC, highlighting its significance as a potential therapeutic target. Therefore, we explored whether HELLPAR influences NPC progression by modulating the miR-448/ADAM10 axis, providing new insights into its underlying molecular mechanisms.

Consistent with prior findings in glioma [23], we observed that HELLPAR was significantly overexpressed in both NPC tissues and cell lines. Importantly, high HELLPAR expression was associated with poorer prognosis in NPC patients, suggesting that HELLPAR may serve as a prognostic indicator. Functional experiments further demonstrated that HELLPAR knockdown inhibited NPC cell proliferation and invasion while promoting apoptosis. In parallel, previous articles have revealed that miR-448 is lowly expressed in lung adenocarcinoma and PDAC tissues and cell lines [14, 26], which aligns with our findings of reduced miR-448 expression in NPC tissues and cells. Moreover, ADAM10 was distinctly elevated in NPC, also consistent with earlier reports [15]. We further confirmed that miR-448 targeted and regulated ADAM10.

One particularly noteworthy aspect of our study is the discovery that HELLPAR acts as a ceRNA, sponging miR-448 to regulate ADAM10 expression. Subcellular localization analysis showed that HELLPAR predominantly resides in the cytoplasm, supporting its role as a ceRNA. Bioinformatic predictions via StarBase identified binding sites between HELLPAR and miR-448, which were subsequently validated through dual-luciferase, RIP, and RNA pull-down assays, confirming their direct interaction. Notably, HELLPAR overexpression suppressed miR-448 levels, whereas miR-448 overexpression reversed the tumor-promoting effects of HELLPAR on NPC cell proliferation and invasion. Conversely, ADAM10 overexpression counteracted the suppressive effects of miR-448, suggesting that HELLPAR may promote NPC progression by regulating the miR-448/ADAM10 axis. Our findings are supported by previous research indicating an inverse relationship between miR-448 and ADAM10 in gastric cancer [14]. Guo et al. have also reported that miR-448 upregulation impedes the abilities of invasion, colony formation, and migration of HCC cells [13]. Similarly, upregulation of miR-448 in glioma U87 cells has been shown to reduce proliferation and induce apoptosis, causing G1/S cell cycle arrest, whereas its inhibition produces the opposite effect [27]. These data suggest that miR-448 broadly functions as a tumor suppressor. In support of this, suppression of ADAM10 has been shown to inhibit proliferation, invasion, and migration in HepG2 cells [28]. as well as to induce growth arrest in mantle cell lymphoma cells [29]. Additionally, overexpressed ADAM10 has been found to protect HCC cells from doxorubicin-induced apoptosis [30].

In summary, this study demonstrates that HELLPAR promotes NPC progression by sponging miR-448, thereby relieving repression on ADAM10. Interfering with HELLPAR leads to increased miR-448 expression, which in turn downregulates ADAM10 and suppresses malignant phenotypes in NPC cells. These findings highlight the HELLPAR/miR-448/ADAM10 axis as a potential therapeutic target in NPC. However, further mechanistic studies and in vivo validations are needed to fully elucidate this regulatory network and identify additional diagnostic biomarkers and therapeutic strategies for NPC.

Author contributions W.J.Z. and Q.Y. finished the study design, H.J.Y. and M.T.Q. finished the experimental studies, Y.J. finished the data analysis, J.Y.L. finished the manuscript editing. All authors read and approved the final version of the manuscript.

Funding The work was not funded by any funding.

Data availability The experimental data used to support the findings of this study are available from the corresponding author upon request.

Declarations

Ethics approval and consent to participate The study conformed to the principles expressed in the *Declaration of Helsinki* and was approved by the Institutional Review Board of Zhangjiagang Hospital Affiliated to Soochow University (Zhang Jiagang First Peoples Hospital). All patients provided written informed consent.Ethics approval and consent to participate.

Competing interests The authors declare no competing interests.

References

1. Wotman M, et al. The prognostic role of programmed death-ligand 1 in nasopharyngeal carcinoma. Laryngoscope. 2020;130(11):2598–606.
2. Wu Q, et al. Cost-effectiveness analysis of gemcitabine plus cisplatin versus docetaxel, cisplatin and fluorouracil for induction chemotherapy of locoregionally advanced nasopharyngeal carcinoma. Oral Oncol. 2020;103: 104588.
3. Young LS. A novel Epstein-Barr virus subtype associated with nasopharyngeal carcinoma found in South China. Cancer Commun (Lond). 2020;40(1):60–2.
4. Yu JY, et al. Quantitative analysis of DCE-MRI and RESOLVE-DWI for differentiating nasopharyngeal carcinoma from nasopharyngeal lymphoid hyperplasia. J Med Syst. 2020;44(4):75.
5. Alterio D, et al. Mixed-beam approach in locally advanced nasopharyngeal carcinoma: IMRT followed by proton therapy boost versus IMRT-only. Evaluation of toxicity and efficacy. Acta Oncol. 2020;59(5):541–8.
6. Han JB, et al. MiR-214 mediates cell proliferation and apoptosis of nasopharyngeal carcinoma through targeting both WWOX and PTEN. Cancer Biother Radiopharm. 2020;35(8):615–25.
7. Tang Y, He X. Long non-coding RNAs in nasopharyngeal carcinoma: biological functions and clinical applications. Mol Cell Biochem. 2021;476(9):3537–50.
8. Ganapathy K, et al. Anticancer function of microRNA-30e is mediated by negative regulation of HELLPAR, a noncoding macroRNA, and genes involved in ubiquitination and cell cycle progression in prostate cancer. Mol Oncol. 2022;16(16):2936–58.
9. Panagal M, et al. Dissecting the role of miR-21 in different types of stroke. Gene. 2019;681:69–72.
10. Chong H, et al. The PGC-1alpha/NRF1/miR-378a axis protects vascular smooth muscle cells from FFA-induced proliferation, migration and inflammation in atherosclerosis. Atherosclerosis. 2020;297:136–45.
11. Selvakumar SC, et al. The emerging role of microRNA-based therapeutics in the treatment of preeclampsia. Placenta. 2024;158:38–47.
12. Selvakumar SC, Preethi KA, Sekar D. MicroRNA-510-3p regulated vascular dysfunction in preeclampsia by targeting vascular endothelial growth factor A (VEGFA) and its signaling axis. Placenta. 2024;153:31–52.
13. Guo JC, et al. microRNA-448 inhibits stemness maintenance and self-renewal of hepatocellular carcinoma stem cells through the MAGEA6-mediated AMPK signaling pathway. J Cell Physiol. 2019;234(12):23461–74.
14. Wu X, et al. miR-448 suppressed gastric cancer proliferation and invasion by regulating ADAM10. Tumour Biol. 2016;37(8):10545–51.
15. You B, et al. Effects of ADAM10 upregulation on progression, migration, and prognosis of nasopharyngeal carcinoma. Cancer Sci. 2015;106(11):1506–14.
16. Wang S, et al. LncRNA MALAT1 promotes oxygen-glucose deprivation and reoxygenation induced cardiomyocytes injury through sponging miR-20b to enhance beclin1-mediated autophagy. Cardiovasc Drugs Ther. 2019;33(6):675–86.
17. Wang D, et al. Depletion of histone demethylase KDM5B inhibits cell proliferation of hepatocellular carcinoma by regulation of cell cycle checkpoint proteins p15 and p27. J Exp Clin Cancer Res. 2016;35:37.
18. Huang Y, et al. MicroRNA-222 promotes invasion and metastasis of papillary thyroid cancer through targeting protein phosphatase 2 regulatory subunit B alpha expression. Thyroid. 2018;28(9):1162–73.
19. Qiu K, et al. Silencing of DJ-1 reduces proliferation, invasion, and migration of papillary thyroid cancer cells in vitro, probably by increase of PTEN expression. Int J Clin Exp Pathol. 2019;12(6):2046–55.
20. Yang D, et al. N6-Methyladenosine modification of lincRNA 1281 is critically required for mESC differentiation potential. Nucleic Acids Res. 2018;46(8):3906–20.
21. Wang ZY, Duan Y, Wang P. SP1-mediated upregulation of lncRNA SNHG4 functions as a ceRNA for miR-377 to facilitate prostate cancer progression through regulation of ZIC5. J Cell Physiol. 2020;235(4):3916–27.
22. Shen S, et al. Silencing lncRNA AGAP2-AS1 Upregulates miR-195-5p to Repress Migration and Invasion of EC Cells via the Decrease of FOSL1 Expression. Mol Ther Nucleic Acids. 2020;20:331–44.
23. Zhu H, et al. HELLPAR/RRM2 axis related to HMMR as novel prognostic biomarker in gliomas. BMC Cancer. 2023;23(1):125.
24. Zhou Y, et al. Micro ribonucleic acid-448 regulates zinc finger e-box binding homeobox 1 to inhibit the growth of breast cancer cells and increase their sensitivity to chemotherapy. Clinics (Sao Paulo). 2022;77: 100089.
25. Nami B, Wang Z. A non-canonical p75HER2 signaling pathway underlying trastuzumab action and resistance in breast cancer. Cells. 2024. https://doi.org/10.3390/cells13171452.
26. Deng J, et al. Long non-coding RNA OIP5-AS1 functions as an oncogene in lung adenocarcinoma through targeting miR-448/Bcl-2. Biomed Pharmacother. 2018;98:102–10.
27. Su HY, et al. MiR-448 downregulates CTTN to inhibit cell proliferation and promote apoptosis in glioma. Eur Rev Med Pharmacol Sci. 2018;22(12):3847–54.

28. Liu S, et al. Silencing ADAM10 inhibits the in vitro and in vivo growth of hepatocellular carcinoma cancer cells. Mol Med Rep. 2015;11(1):597–602.
29. Armanious H, et al. Constitutive activation of metalloproteinase ADAM10 in mantle cell lymphoma promotes cell growth and activates the TNFalpha/NFkappaB pathway. Blood. 2011;117(23):6237–46.
30. Yang CL, et al. ADAM10 overexpression confers resistance to doxorubicin-induced apoptosis in hepatocellular carcinoma. Tumour Biol. 2012;33(5):1535–41.